Stability of the Perforated Layer (PL) Phase in Diblock Copolymer Melts

Damian A. Hajduk,* Hiroshi Takenouchi, Marc A. Hillmyer, and Frank S. Bates*

Department of Chemical Engineering and Materials Science, University of Minnesota, Minneapolis, Minnesota 55455

Martin E. Vigild and Kristoffer Almdal

Risø National Laboratory, DK-4000 Roskilde, Denmark

Received November 13, 1996; Revised Manuscript Received April 23, 1997[⊗]

ABSTRACT: We reexamine the stability of hexagonally modulated layer (HML) and hexagonally perforated layer (HPL) morphologies in a number of block copolymer systems of low to moderate molecular weight. Using small-angle X-ray scattering and dynamic mechanical spectroscopy, we show that these structures are long-lived nonequilibrium states which convert to the bicontinuous gyroid (G) morphology upon isothermal annealing. Comparison of phase transition kinetics across chemically distinct systems spanning a wide range of molecular weights and monomeric friction coefficients reveals a composition dependence to these dynamics. This suggests effects associated with the mobility of individual chains are of lesser importance in explaining the apparent metastability of the HML and HPL structures; instead, the composition dependence of the transition mechanism appears to dominate the observed behavior. The revised phase behavior for these materials is in excellent agreement with mean-field predictions for diblock copolymer melts.

Introduction

Block copolymers are known for the variety of ordered morphologies that can form upon microphase separation.[1−3] Mean-field theories predict this behavior as a function of the degree of segregation of the system (χN), the volume fraction occupied by one of the blocks (f), and the conformational asymmetry of the blocks (ϵ).[4,5] Selection of a given copolymer chemistry fixes ϵ and (in theory) restricts the phase behavior to depend solely on χN and f. In the microphase-separated state, early theories predicted only the three "classical" morphologies—lamellae (L), cylinders (C), and spheres (S)—to be stable.

Experiments have recently revealed three additional "complex" phases—hexagonally modulated layers (HML),[6] hexagonally perforated layers (HPL),[6,7] and the gyroid (G)[8,9]—in a narrow range of volume fractions and segregations separating the lamellar and cylindrical morphologies. The HML phase consists of alternating minority and majority component layers in which the thickness of the minority component domains is modulated with a hexagonal in-plane symmetry. In the HPL phase, hexagonally packed channels of majority component material extend through the minority component layers to form a monocontinuous structure. (A similar morphology has been identified in blends of diblock copolymers with homopolymers, where it is known as the lamellar-catenoid (LC) morphology.)[10,11] The stacking of the HML modulations and the HPL channels is at present unknown; the experimental data are consistent with both *abab*... and *abcabc*... arrangements. The G phase is formed from two distinct, interpenetrating networks of the minority component chains which are embedded in a matrix of majority component material. The resulting tricontinuous structure was initially misidentified as the ordered bicontinuous double diamond (OBDD) morphology[12,13] and is occasionally identified by its space group ($Ia\bar{3}d$).

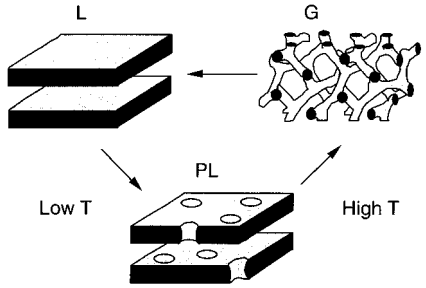

Figure 1. Schematics of the minority component domains in the lamellar (L), perforated layer (PL), and gyroid (G) morphologies. Arrows indicate the direction of experimentally observed morphological transitions as described in the text.

Current theory accounts for the appearance of the G phase as well as the absence of the OBDD structure.[14−19] Although the HML and HPL structures are also predicted to be nonequilibrium morphologies,[18−22] the HPL phase is most nearly in equilibrium at compositions (f) and segregations (χN) where it is observed experimentally, and so its absence from calculated phase diagrams might reflect deficiencies in theoretical models. In an attempt to identify the physical characteristics which might underlie such deficiencies, we have reexamined the phase behavior of a large number of block copolymers previously identified as possessing the HPL morphology. Here, we report our findings concerning the stability of this microstructure, focusing on materials displaying transitions between the L, HPL, and G morphologies (Figure 1).

Experimental Methods

The synthesis and initial morphological characterization of the polymers used in this study have been described in detail elsewhere (see Table 1). Films of polystyrene−polyisoprene (PI−PS) diblocks containing 0.5 wt % Irganox 1010 as an antioxidant were prepared through solvent casting from toluene followed by vacuum drying for 1 day at 20 °C and 3

* To whom correspondence should be addressed.
[⊗] Abstract published in *Advance ACS Abstracts,* June 1, 1997.

S0024-9297(96)01673-7 CCC: $14.00

Table 1. Molecular Characteristics and Previously Reported Phase Behavior[a]

sample name	f	M_n	phases and transition temperatures reported previously (°C)
		Polyethylene−Poly(ethylethylene) (PE−PEE)[23−25]	
EE-5D	0.65	36.0	H(M/P)L-(127) → C-(164) → dis
EE-6D[b]	0.65	43.0	L-(138) → HML-(175) → HPL-(180) → C-(202) → dis
EE-6H[b]	0.65	43.0	L-(143) → HML-(177) → HPL-(184) → C-(204) → dis
EE-12H	0.67	40.0	L-(133) → HPL-(175) → C-(275) → dis
EE-7H[c]	0.75	44.0	L-(148) → dis
EE-17D[c]	0.60	42.0	C-(242) → dis
		Polyisoprene−Polystyrene (PI−PS)[26,27]	
IS-39	0.39	31.5	HPL-(175) → G-(234) → dis
IS-65	0.65	39.5	L-(190) → HPL-(221) → G-(279) → dis
IS-66	0.66	39.7	L-(159) → HPL-(210) → G-(268) → dis
IS-68	0.68	39.9	L-(134) → HPL-(198) → G-(252) → C-(267) → dis
		Polystyrene−Poly(2-vinylpyridine) (PS−PVP)[28]	
SV-8	0.38	20.2	HPL-(146) → G-(180) → dis
SV-9	0.65	20.5	HPL-(175) → dis
		Poly(ethylene-*co*-propylene)−Poly(dimethylsiloxane) (PEP−PDMS)[29,30]	
PEP−PDMS 7	0.64	10.4	L-(115) → G-(160) → dis
PEP−PDMS 12	0.68	11.5	(no data reported)
		Poly(ethylene oxide)−Poly(ethylethylene) (PEO−PEE)[31,32]	
OE-5[c]	0.70	8.4	L-(104) → PL-(166) → G-(242) → dis
OE-10[c]	0.72	8.7	L-(147) → PL-(180) → G-(217) → C-(260) → dis

[a] f, volume fraction of the block given first in the name for the copolymer and possessing the lower value of R_g^2/V, where R_g is the radius of gyration and V is the block volume; M_n, number average molecular weight in kg/mol; L, lamellar; HML, hexagonally modulated layers; HPL, hexagonally perforated layers; G, gyroid; C, hexagonally packed cylinders; dis, disordered phase. H(M/P)L denotes a rheological response consistent with both HML and HPL. [b] EE-6D and -6H were created through saturation of the corresponding polybutadiene copolymers with D_2 and H_2 gas, respectively. [c] Identifies polymers used to form binary blends as described in the text.

days at 110 °C prior to use. Films of IS-65 and IS-66 without antioxidant were prepared through melt pressing into sheets 0.5 mm thick in vacuum at 120 °C in order to test for changes in phase behavior associated with either the presence of antioxidant or the solvent-casting process. Comparison of rheological behavior obtained in samples prepared by the two methods revealed no experimentally significant differences. Films of polyethylene−poly(ethylethylene) (PE−PEE) and polystyrene−poly(2-vinylpyridine) (PS−PVP) copolymers were prepared through melt pressing of precipitated material, as described elsewhere,[22,24] followed by slow cooling to room temperature. Samples of poly(ethylene oxide)−poly(ethylethylene) (PEO−PEE) copolymers were prepared by melt pressing at 50 °C followed by crystallization of the PEO block at room temperature. This resets the sample morphology to a randomly oriented, semicrystalline lamellar phase,[30] minimizing the effect of nonequilibrium morphologies arising from sample preparation. Poly(ethylene-*co*-propylene)−polydimethylsiloxane (PEP−PDMS) copolymers were used as recovered from polymerization.

Blends of PEO−PEE copolymers were prepared through solvent casting from tetrahydrofuran (THF), followed by vacuum drying at 20 °C prior to use. Blends of PE−PEE copolymers were prepared through codissolution in toluene at 90 °C, followed by precipitation in methanol at room temperature and melt pressing at 120 °C into sheets 0.5 mm in thickness. Blends of PEP−PDMS copolymers were prepared through codissolution in *n*-hexane followed by evaporation of the solvent. Blends of polymers closely matched in composition and molecular weight are expected to mimic the phase behavior of the corresponding neat copolymer,[24,32] providing an alternate route to identifying composition-dependent phase behavior.

Viscoelastic characteristics were measured on a Rheometrics RSA-II rheometer using a reciprocating parallel plate geometry with sample thicknesses of 0.3 or 0.5 mm. A nitrogen purge was used to minimize oxidative degeneration at high temperatures. PS−PI samples were cut from films prepared as described above and mounted on the rheometer plates at 80 °C. After heating to 110 °C under nitrogen, the gap thickness was adjusted to 0.5 mm and the plates were cooled to room temperature in order to remove any excess material. PE−PEE samples were mounted at room temperature, heated to 120 °C for adjustment of the gap thickness, and then cooled to 20 °C for removal of excess polymer before starting measurements. PEO−PEE samples were melted at 50 °C and placed on the rheometer plates. After adjusting the gap thickness, excess material was removed and the polymer was permitted to recrystallize at 10 °C prior to beginning measurements. PEP−PDMS copolymers were mounted on the plates at 20 °C prior to use. Isothermal frequency sweeps measured the elastic (G') and loss (G'') moduli at a constant temperature over frequencies (ω) from 0.1 to 100 rad/s; temperature sweeps monitored $G'(T)$ and $G''(T)$ at frequencies from 0.1 to 1.0 rad/s while scanning at rates from 0.1 to 10 °C/min. Strain amplitudes of 1% were employed unless otherwise indicated. Size exclusion chromatography (SEC) performed on selected specimens after these measurements revealed negligible degradation of the material. Comparison of multiple temperature scans from the same sample of selected PEO−PEE, PI−PS, or PEP−PDMS materials revealed no changes in moduli or phase transition temperatures, indirectly confirming this result.

Small-angle X-ray scattering (SAXS) measurements were conducted on a small-angle beamline constructed at the University of Minnesota. Cu Kα X-rays were generated by a Rigaku RU-200BVH rotating anode X-ray machine equipped with a 0.2 × 2 mm^2 microfocus cathode and Franks mirror optics. Unsheared samples were placed inside an evacuated sample chamber and maintained at the appropriate temperature by a pair of heaters mounted on a water-cooled brass block (temperature range 5−260 °C, stability ±0.1 °C). Samples annealed for more than 24 h were sealed in evacuated ampules and immersed in an oil bath at the desired temperature. Upon removal from the bath, samples were quenched in liquid nitrogen prior to extraction from the ampule. Size exclusion chromatography (SEC) revealed negligible degradation of the annealed material. Two-dimensional diffraction images were collected with a multiwire area detector (HI-STAR, Siemens Analytical X-ray Instruments) and corrected for detector response characteristics prior to analysis. Integration times ranged from 60 to 3600 s, depending on the electron density contrast characteristic of the specimen. Images were converted to one-dimensional formats by integrating azimuthally along an arc ±20° from the horizontal axis.

Results and Discussion

In general, rheological data for all polymers reproduced those obtained previously.[23−31] Preliminary phase

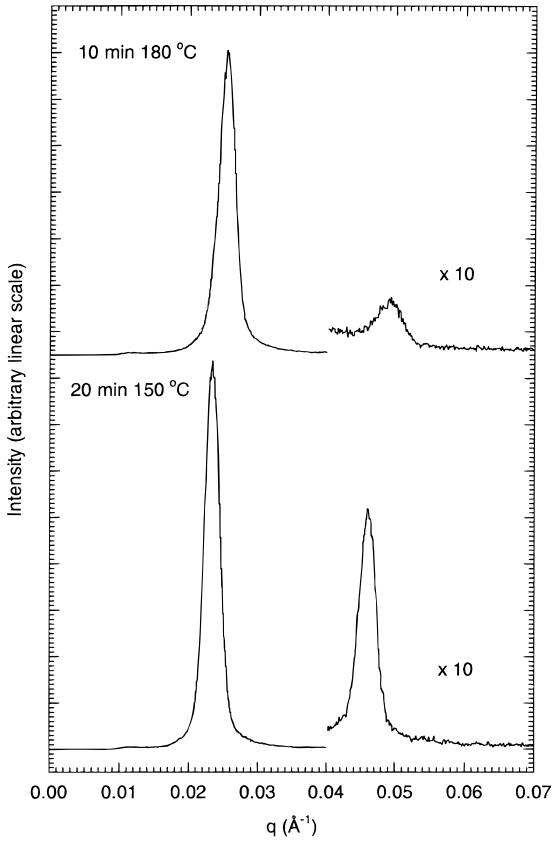

Figure 2. Diffraction characteristic of the L and PL morphologies, recorded from a melt-pressed sample of IS-66. Prior rheological measurements and transmission electron microscopy indicate a transition from the lamellar (L) to the hexagonally perforated layer (HPL) phase upon heating through 159 °C.[21] After annealing for 20 min at 150 °C, sharp reflections appear at position ratios of 1:2, indicative of a lamellar morphology. Subsequent annealing for 10 min at 180 °C, which induces a transition to the HPL structure that can be detected through rheology, produces significant increases in the widths of the first two peaks without generating additional reflections in this unsheared material. Diffraction which can be associated with a particular in-plane arrangement of the majority component channels is not observed. This second morphology is therefore denoted "perforated layers", or PL. The similarities in diffraction signature preclude differentiation of *unsheared* L and PL morphologies through scattering methods alone.

assignments were made by comparing viscoelastic frequency response spectra with those obtained previously in systems of known microstructure.[24] SAXS from unsheared specimens confirmed these assignments for the lamellar, cylindrical, and gyroid morphologies. Lamellar (L) phases were characterized by peaks spaced at reciprocal space position ratios of 1:2:3:.... Gyroid (G) phases were identified by peaks at ratios of $\sqrt{3}$:$\sqrt{4}$, with occasional reflections at higher position ratios, as expected for the $Ia\bar{3}d$ space group. Samples exhibiting this morphology frequently developed a grain structure containing a small number of large, highly oriented domains, resulting in a "spotty" appearance to the diffraction image.[8,29] This appears to be a general feature of the G phase.

Specimens with microstructures previously identified as HML or HPL produced lamellar-like diffraction with broad reflections and relatively few higher order peaks, indicating a lack of long-range order; see Figure 2. Typical images from unsheared material (either solvent cast or melt pressed) showed a single, sharp reflection with weak maxima spaced at 180° in azimuthal angle. This suggests a layered structure in which the layers orient preferentially in the plane of the film. Higher order reflections at position ratios of 1:2 were frequently, though not always, observed. Previously published electron micrographs of unsheared PS−PVP samples have demonstrated the presence of majority component channels extending through the minority component layers in these samples without revealing a hexagonal in-plane packing.[28] Consistent with these micrographs, no features in SAXS data from PE−PEE, PI−PS, and PS−PVP specimens previously identified as HPL could be associated with an ordering of the majority component channels. Diffraction from the PEO−PEE copolymer OE-10 showed two faint reflections at an approximate position ratio of 1:$\sqrt{2}$ in addition to that associated with the layers themselves. This suggests that the channels do not acquire long-range order in the absence of a shear field except perhaps in systems of extremely low molecular weight. Similar layerlike diffraction was recorded from unsheared samples previously identified as exhibiting the HML morphology. We therefore denote these structures "modulated layers" (MLs) and "perforated layers" (PLs) in order to emphasize the shear-induced origin of the in-plane long-range order. As the scattering signature of the PL state was not sufficient to differentiate the sample microstructure from the L phase, identification of this morphology was based primarily on its rheological signature in combination with previously published SANS and TEM measurements.

The PL state is a nonequilibrium structure in these copolymers. Prolonged isothermal annealing converted it to the G phase in all of the systems examined. Both rheological and scattering data show evidence of this behavior; see Figure 3. The time required for this transition ranged from several hours to 31 days, depending on the composition and molecular weight of the material and the proximity of the annealing temperature to the highest glass transition present in the system. It appears that the pronounced metastability of the PL state, relative to that of the (more stable) G phase, led to its misidentification as an equilibrium morphology. After formation of the cubic phase, no further transitions were observed *via* SAXS upon continued isothermal annealing. Attempts to recover the PL state by cooling the G phase to temperatures at which the former was observed in rheological measurements were unsuccessful. We speculate that prior reports of G → PL transitions, in which coexisting PL and G structures were observed *via* transmission electron microscopy (TEM),[27] actually reflected incomplete conversion of the initial, nonequilibrium PL phase to the G morphology.

In polymers exhibiting only complex ordered phases (SV-8, SV-9, and IS-39), the PL structure appears to be an artifact induced by the sample preparation process. All three polymers formed poorly ordered, layered structures upon casting from a nonselective, good solvent followed by brief annealing slightly above the highest glass transition temperature present in the system (∼100 °C). Similar diffraction was recorded from films prepared by melt pressing of precipitated material. Both preparation methods produced layers with a preference for orienting in the plane of the film, indicating that surface (and/or flow) fields influenced the sample microstructure. Subsequent low-temperature annealing (at 120 °C) produced transformations to the G phase, as described above. Samples prepared by

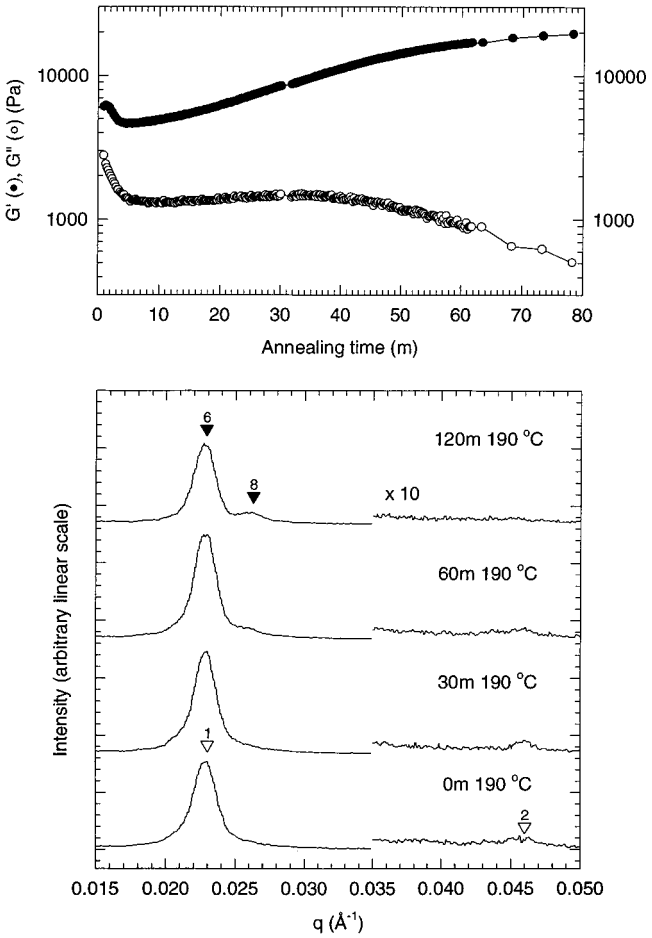

Figure 3. PL → G transition observed upon annealing the polyisoprene−polystyrene copolymer IS-68 at 190 °C. Prior rheological data identified this transition as occurring at 198 °C.[27] Over 80 min, the viscoelastic response (top; measured at $\gamma = 1\%$, $\omega = 1$ rad/s) evolves continuously from a modulus characteristic of PL to a higher, elastically dominated response characteristic of the G phase. For comparison, an isochronal temperature scan of this material appears in Figure 4. Small-angle scattering measurements of unsheared material (bottom) reveal a simultaneous evolution from a poorly ordered layered structure to the G morphology. Open arrows indicate layered peaks at position ratios of 1:2; filled arrows indicate G phase reflections at position ratios of $\sqrt{6}$:$\sqrt{8}$. Similar microstructural evolution occurs at lower temperatures, though at a much slower rate; this transition requires at least 14 h at 175 °C and was confirmed after 28 days at 150 °C.

disordering and quenching in liquid nitrogen—a technique which minimizes these surface and flow effects—did not exhibit diffraction indicative of any well-ordered structure prior to the appearance of the G morphology during *in situ* annealing. These findings suggest that the cubic phase is the only equilibrium ordered morphology in these three materials.

In the other systems, the PL structure appears to facilitate the L → G transition. Although a detailed discussion of this mechanism is beyond the scope of this article, we note that both the HPL structure proposed on the basis of SANS measurements and the currently accepted model for the G morphology are composed of minority component domains which can be constructed from arrangements of (nearly identical) planar, threefold-coordinated structural elements.[6,26] Despite this similarity in local structure, the overall arrangement of these elements in the HPL state retains a planar aspect reminiscent of the L phase, in contrast to the three-dimensional interpenetrating networks formed in the G morphology. This combination of L-like and G-like characteristics presumably underlies the intermediary role played by the PL morphology and may account for its appearance during sample preparation. This also accounts for the apparent metastability of the PL phase: since the HPL and G morphologies possess nearly identical local structures, the difference in free energy which drives the PL → G relaxation is extremely small. Recent theory indicates that such a perforated lamellar structure with hexagonal in-plane symmetry might form as a transient structure during transitions out of a thermodynamically unstable lamellar phase.[34−37]

Confirmation of the equilibrium nature of the low-temperature lamellar phase is complicated by the slow kinetics characteristic of polymeric materials. Nonequilibrium structures formed during sample preparation or as a consequence of a phase transition mechanism are easily misinterpretable as stable mesophases, as was apparently the case with the PL state. Perhaps the most reliable (though not an absolute) means to detect such metastable structures is to demonstrate the reversibility of all transitions between ordered morphologies. The relaxation of a nonequilibrium structure is in principle an irreversible process, while transitions between equilibrium states should be thermally reversible.

An alternative procedure is to quench initially disordered materials to a particular temperature and follow the evolution of the sample morphology with an *in situ* technique. This quenching can be performed through immersion in liquid nitrogen or through precipitation of a dilute copolymer solution, as was done in preparation of the PE−PEE blends. This approach implicitly assumes that any kinetic barriers to achieving equilibrium arise from the rearrangement of the microphase-separated interface and are presumably minimized during ordering from a disordered phase. Unfortunately, the process by which this occurs remains poorly understood, and it is not obvious that this method will always yield an equilibrium microstructure instead of first producing a (kinetically trapped) nonequilibrium state. Even in the absence of such intermediates, the presence of surface or flow fields might influence the ordering process and drive the copolymer to adopt a nonequilibrium morphology. These limitations restrict the usefulness of this approach.

Comparison of rheologically measured phase behaviors for each system reveals a composition dependence to the transition kinetics which complicates the identification of equilibrium morphologies. For example, in the PI−PS copolymers reviewed here, cooling the G phase below the point at which the L → PL transition was observed upon heating did not always return the sample to the L phase. Full thermoreversibility was achieved only in IS-65, which has a composition placing it at the lamellar edge of the complex phase window. Both rheological and SAXS measurements indicate that after the G phase is formed, the L phase reappears only after cooling below the point at which the L → PL transition is observed (rheologically) upon heating; see Figure 4. In (more asymmetric) IS-66 and IS-68, the cubic phase persisted down to the highest glass transition temperature present in the system even when extended annealing times (14 days) were used. Hajduk *et al.*[8] have demonstrated a reversible L → G transition in a polyisoprene−polystyrene copolymer, denoted SI 10/17, with a composition nominally resembling that of IS-66 but of lower molecular weight. Although our inabil-

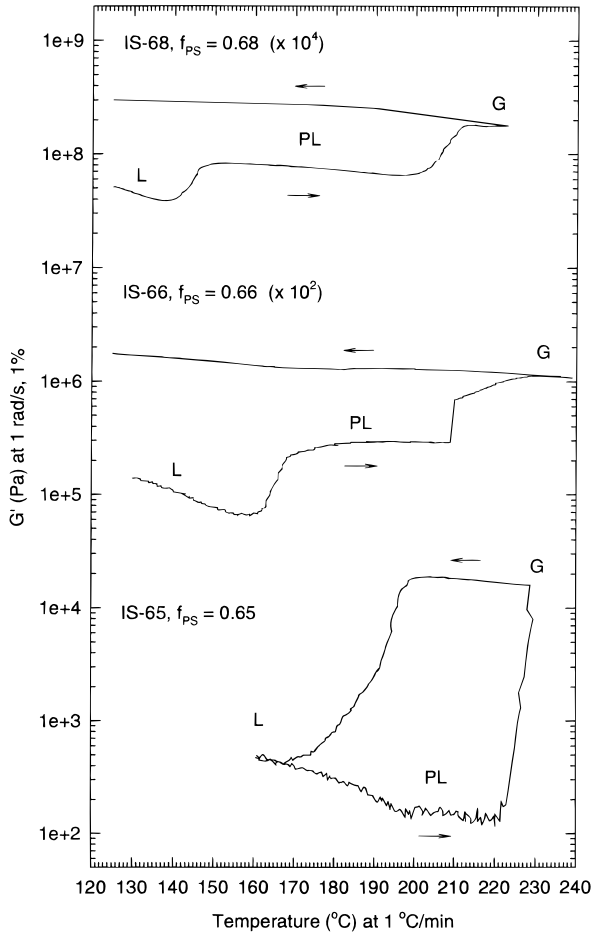

Figure 4. Viscoelastic storage (G') modulus at 1 rad/s, 1% strain, and a temperature ramp rate of 1 °C/min for three polyisoprene−polystyrene copolymers with roughly equal molecular weights but different polyisoprene volume fractions. Arrows indicate the direction of temperature change. Sudden changes in the magnitude or slope of $G'(T)$ are generally associated with order−order transitions; this has been confirmed *via* SAXS in the materials shown. L, PL, and G identify lamellar, perforated layer, and gyroid morphologies, respectively. In (thermoreversible) IS-65, the L → PL transition temperature measured upon heating is roughly coincident with the G → L transition temperature observed upon cooling, consistent with the nonequilibrium nature of the PL state. (Identification of the PL structure is somewhat tentative, owing to the small magnitude of the change in $G'(T)$ at the L → PL transition; electron microscopy indicates coexisting but poorly ordered L and PL phases at this point.) The irreversibility of the L → PL → G transition in IS-66 and IS-68 is ascribed to a composition-dependent transition rate, as described in the text.

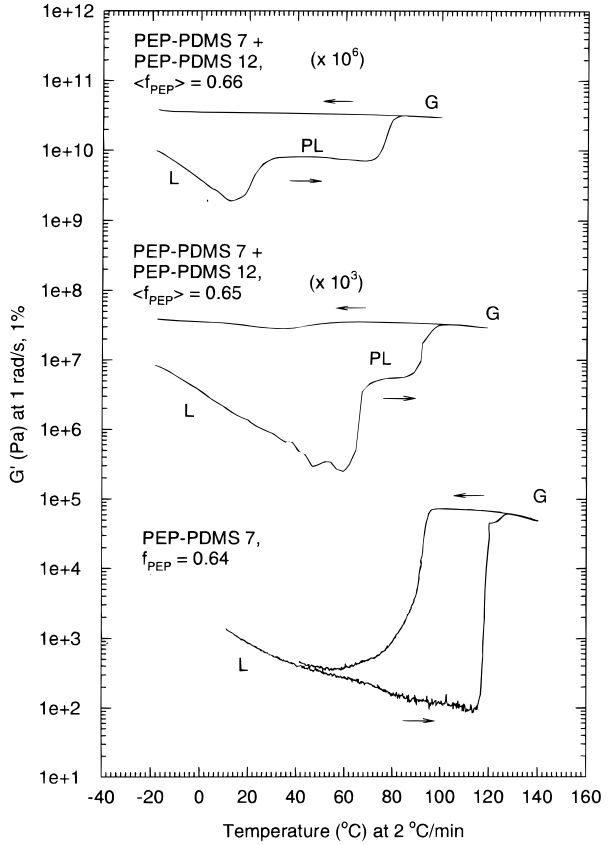

Figure 5. Viscoelastic storage (G') modulus at 1 rad/s, 1% strain, and a temperature ramp rate of 2 °C/min for three poly(ethylene-*co*-propylene)−poly(dimethylsiloxane) (PEP−PDMS) materials. Arrows indicate the direction of temperature change. L, PL, and G identify lamellar, perforated layer, and gyroid morphologies, respectively. As in the PI−PS system, the L → G transition becomes increasingly difficult to thermoreverse as the asymmetry of the system increases.

ity to reverse the transition in IS-66 might be due to a molecular weight dependence in the transition kinetics, the uncertainty in composition between these two materials is sufficiently large ($\Delta f \sim 0.01$) that the behavior observed in SI 10/17 might be more comparable to that observed in (fully reversible) IS-65.

Suggestive evidence for the equilibrium nature of the lamellar phase in IS-66 and IS-68 comes from samples which were disordered at 280 °C prior to quenching in liquid nitrogen. Scattering recorded at room temperature exhibited a single broad maximum characteristic of the disordered state. Subsequent *in situ* annealing for 5 min at 120 °C produced well-resolved peaks at spacing ratios of 1:2:4 (IS-66) and 1:2 (IS-68), indicating the formation of lamellar phases and suggesting that the G phase is not in equilibrium at these low temperatures. No further changes were observed in these polymers after 2 h of further annealing.

Rheological and scattering measurements for other copolymers indicate comparable kinetics. An inability to reverse the L → G transition except at the lamellar edge of the complex phase window has been observed in PEP−PDMS[30] (Figure 5), and PE−PEE (Figure 6) copolymers. Although PEO−PEE copolymers[31] show similar rheological behaviors (Figure 7), small-angle scattering has confirmed the reappearance of the lamellar phase in OE-10, the most asymmetric PEO−PEE copolymer, after extended annealing at low temperatures. The hysteresis loops associated with the phase behavior of the thermally reversible systems collapse upon reducing the temperature scan rate, providing further evidence for the equilibrium nature of the lamellar and gyroid phases in these specimens (Figure 8). The appearance of qualitatively identical behaviors in copolymers spanning a wide range of molecular weights, degrees of entanglement, and monomeric friction coefficients suggests that effects associated with the motion of individual chains are of comparatively minor importance. Instead, the composition dependence of the transition mechanism appears to be the controlling factor.

Whether the irreversibility of the L → G transition arises from the nonequilibrium nature of the lamellar phase, or instead reflects composition-dependent variations in the G → L transition rate is unclear. The quench experiments on IS-66 and IS-68 suggest that the

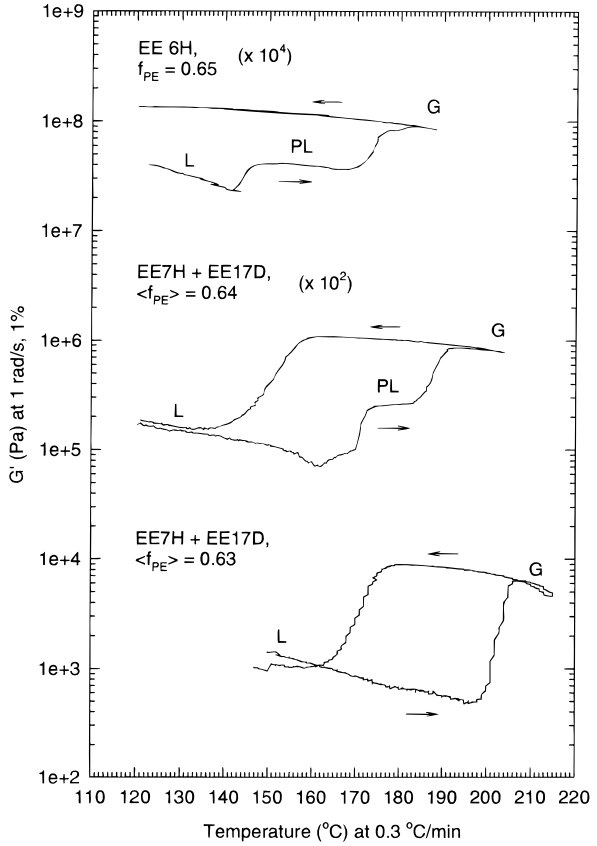

Figure 6. Viscoelastic storage (G') modulus at 0.5 rad/s, 1% strain, and a temperature ramp rate of 0.3 °C/min for three polyethylene−poly(ethylethylene) (PE−PEE) materials. Arrows indicate the direction of temperature change. L, PL, and G identify lamellar, perforated layer, and gyroid morphologies, respectively. The presence of qualitatively identical transition kinetics in materials of quite different molecular weight and viscoelastic characteristics suggests that the composition dependence of the transition mechanism dominates the observed phase behavior.

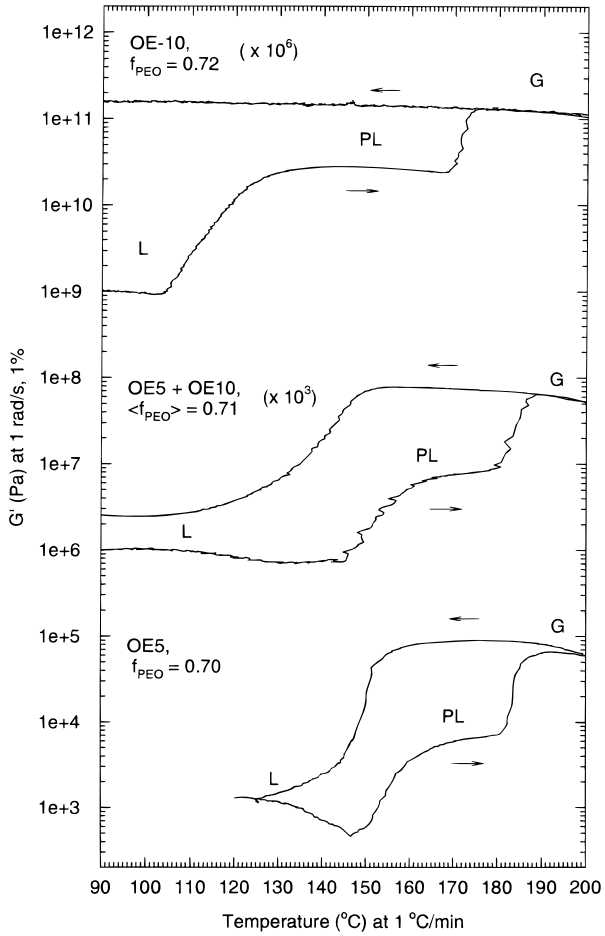

Figure 7. Viscoelastic storage (G') modulus at 1 rad/s, 1% strain, and a temperature ramp rate of 1 °C/min for three poly(ethylene oxide)−poly(ethylethylene) (PEO−PEE) materials. Arrows indicate the direction of temperature change. L, PL, and G identify lamellar, perforated layer, and gyroid morphologies, respectively. (Small-angle measurements in OE-10 indicate that the L−G transition is thermoreversible upon prolonged (12 h) annealing.)

lamellar morphology is in equilibrium at low temperatures, as does the thermoreversibility observed *via* rheology and SAXS in the PEO−PEE materials and the formation of a lamellar phase upon melt pressing of disordered PE−PEE blends. An inability to recover the initial lamellar phase would therefore result from an unusually slow G → L transition rate at certain compositions, consistent with findings in the PEO−PEE system and with previously published experiments on PS−PI materials.[8] However, the aforementioned limitations of the quench technique make this a questionable method for determining equilibrium microstructure. It is certainly possible that the G phase is in equilibrium at a higher degree of segregation than has previously been concluded from experiment, consistent with a recent calculation.[18] In this case, the lamellar phase identified at low temperatures in the thermally irreversible PE−PEE, PS−PI, and PEP−PDMS systems would be an artifactual morphology induced by the flow fields associated with melt pressing, solvent casting, and rheological sample mounting.

The systems reviewed in this work span the compositions at which complex phases appear on both sides of the morphology diagram for PI−PS and PS−PVP copolymers. This suggests that (H)PL is not an equilibrium microstructure in copolymers of moderate molecular weight. Measurements in the PE−PEE system indicate that a similar conclusion holds for the (H)ML structure. Prior work has suggested that ML and PL become increasingly stable (relative to G) as the molecular weight of the system increases.[3] Although this was previously interpreted in terms of fluctuation-dependent influences on complex phase behavior, we now suspect that the apparent stability of the ML and PL structures, and the absence of the G phase, derives from the slow kinetics associated with long, highly entangled chains. The materials reviewed in this work were selected in part to avoid such limitations. In general, the parameter $\bar{N}$, which governs the degree to which fluctuations influence the behavior of the system,[38] is defined by $\bar{N} = Na^6v^{-2}$, where a and v are the length and volume of the N statistical segments composing the polymer. This can be rewritten as $(Na^2)^3/(Nv)^2$, revealing that $\bar{N}$ scales as the square of the mean number of entanglements per chain and demonstrating that fluctuation and entanglement effects are inextricably linked. Experimental differentiation of these influences will therefore be difficult. However, the excellent agreement between the revised morphology diagrams and the mean-field prediction suggests that fluctuation effects are of comparatively minor importance in descriptions of ordered morphologies in block copolymers.

Conclusions

The hexagonally modulated layer (HML) and hexagonally perforated layer (HPL) morphologies, previously

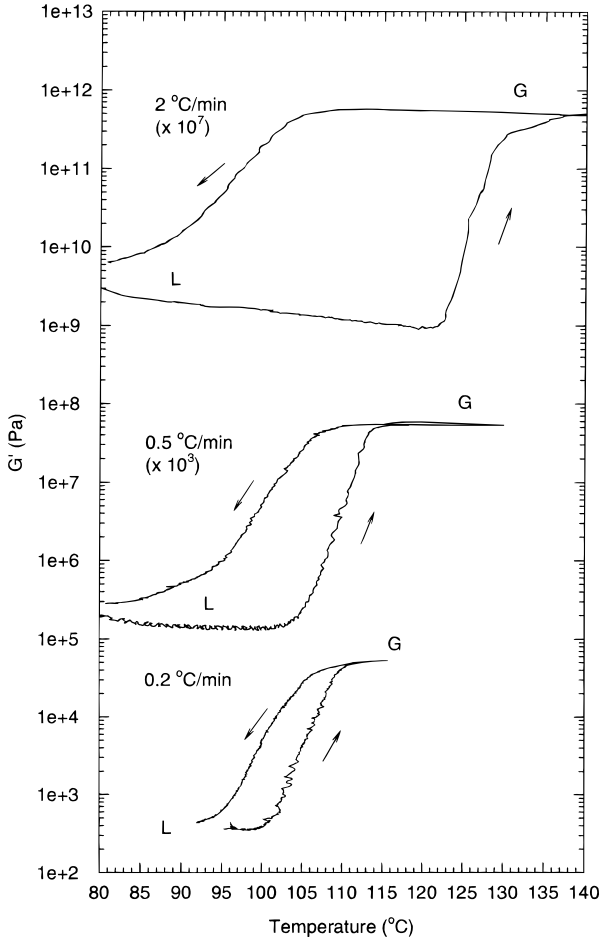

Figure 8. Viscoelastic storage modulus (G') for PEP−PDMS 7 during measurements at three different temperature scan rates ($\gamma = 5\%$, $\omega = 10$ rad/s). Arrows indicate the direction of temperature change. The location of the L → G transition shifts to lower temperatures as the scan rate is reduced, while the temperature at which the G → L transformation takes place upon cooling is unaffected.

identified as equilibrium microstructures in studies of block copolymer phase behavior, have instead been shown to be unusually long-lived nonequilibrium structures involved in the formation of the gyroid (G) phase in a large number of block copolymer systems. The long-range, in-plane hexagonal packing of majority component channels which characterizes the HPL structure results from the application of a shear field. In its absence, the channels exhibit only short-range order at best, and the morphology is known as "perforated layers", or PL.

PL can be induced during the sample preparation process by the application of strong surface or flow fields. The reason for its appearance is unknown but is possibly connected with the unusual structure of the morphology; it combines a threefold-coordinated minority component domain structure similar to that of the G phase with the layered geometry characteristic of the L morphology. Surface fields might favor the development of layered structures, thereby stabilizing the PL structure in a G-forming copolymer during sample preparation. Alternatively, in the event that the transitions described here reflect the existence of thermodynamic stability limits for the lamellar phase (which cannot necessarily be inferred from the experimental data), PL might result from instabilities characteristic of the lamellar morphology.[34−37]

Comparison of several different materials spanning a wide range of molecular weights, monomeric friction coefficients, and number of entanglements per chain has revealed a composition (f) dependence to the G → L transition kinetics, suggesting that the apparent irreversibility of the L → G transition in polymers of moderate molecular weight is not the result of kinetic constraints on molecular motion. Although measurements on quenched polystyrene−polyisoprene diblocks suggest that the lamellar phase is in equilibrium at low temperatures, it is possible that at certain compositions (f), the G phase is in equilibrium at higher degrees of segregation than has previously been believed.

The slow kinetics associated with the PL → G relaxation are expected to be especially severe in highly entangled systems. The absence of the G phase from copolymers of high molecular weight is now thought to arise from these kinetic limitations. Indeed, as dissipation of *any* nonequilibrium effects generated by the sample preparation process might require excessive annealing times, identifying equilibrium microstructures in these systems will be extremely difficult. Preliminary evidence supports this view.[39]

Acknowledgment. We thank M. W. Matsen for useful discussions and R.-M. Ho for electron microscopy of IS-65 and IS-66. Support for this work was provided by the National Science Foundation (Grant DMR-9405101) and by a NATO travel grant to F.S.B. and K.A.

References and Notes

(1) Bates, F. S.; Fredrickson, G. H. *Annu. Rev. Phys. Chem.* **1990**, *41*, 525.
(2) Thomas, E. L.; Lescanec, R. L. *Philos. Trans. R. Soc. London, Ser. A* **1994**, 1.
(3) Bates, F. S.; Schulz, M. F.; Khandpur, A. K.; Förster, S.; Rosedale, J. H.; Almdal, K.; Mortensen, K. *Faraday Discuss.* **1994**, *98*, 7.
(4) Vavasour, J. D.; Whitmore, M. D. *Macromolecules* **1992**, *25*, 5477.
(5) Matsen, M. W.; Schick, M. *Macromolecules* **1994**, *27*, 4014.
(6) Hamley, I. W.; Koppi, K. A.; Rosedale, J. H.; Bates, F. S.; Almdal, K.; Mortensen, K. *Macromolecules* **1993**, *26*, 5959.
(7) Thomas, E. L.; Anderson, D. M.; Henkee, C. S.; Hoffman, D. *Nature* **1988**, *334*, 598.
(8) Hajduk, D. A.; Harper, P. E.; Gruner, S. M.; Honeker, C. C.; Kim, G.; Thomas, E. L.; Fetters, L. J. *Macromolecules* **1994**, *27*, 4063.
(9) Schulz, M. F.; Bates, F. S.; Almdal, K.; Mortensen, K. *Phys. Rev. Lett.* **1994**, *73*, 86.
(10) Disko, M. M.; Liang, K. S.; Behal, S. K.; Roe, R.-J.; Jeon, K. J. *Macromolecules* **1993**, *26*, 2983.
(11) Spontak, R. J.; Smith, S. D.; Ashraf, A. *Macromolecules* **1993**, *26*, 956.
(12) Thomas, E. L.; Alward, D. B.; Kinning, D. J.; Martin, D. C.; Handlin, D. L.; Fetters, L. J. *Macromolecules* **1986**, *19*, 2197.
(13) Hajduk, D. A.; Harper, P. E.; Gruner, S. M.; Honeker, C. C.; Thomas, E. L.; Fetters, L. J. *Macromolecules* **1995**, *28*, 2570.
(14) Matsen, M. W.; Schick, M. *Phys. Rev. Lett.* **1994**, *72*, 2660.
(15) Olmsted, P. D.; Milner, S. T. *Phys. Rev. Lett.* **1994**, *72*, 936; **1995**, *74*, 829.
(16) Milner, S. T. *J. Polym. Sci. B* **1994**, *32*, 2743.
(17) Likhtman, A. E.; Semenov, A. N. *Macromolecules* **1994**, *27*, 3103.
(18) Matsen, M. W.; Bates, F. S. *Macromolecules* **1996**, *29*, 1091.
(19) Matsen, M. W.; Bates, F. S. *Macromolecules* **1996**, *29*, 7641.
(20) Fredrickson, G. H. *Macromolecules* **1991**, *24*, 3456.
(21) Olvera de la Cruz, M.; Mayes, A. M.; Swift, B. W. *Macromolecules* **1992**, *25*, 944.
(22) Hamley, I. W.; Bates, F. S. *J. Chem. Phys.* **1994**, *100*, 6813.
(23) Rosedale, J. H.; Bates, F. S.; Almdal, K.; Mortensen, K.; Wignall, G. D. *Macromolecules* **1995**, *28*, 1429.
(24) Zhao, J.; Majumdar, B.; Schulz, M. F.; Bates, F. S.; Almdal, K.; Mortensen, K.; Hajduk, D. A.; Gruner, S. M. *Macromolecules* **1996**, *29*, 1204.

(25) Hamley, I. W.; Gehlsen, M. D.; Khandpur, A. K.; Koppi, K. A.; Rosedale, J. H.; Schulz, M. F.; Bates, F. S.; Almdal, K.; Mortensen, K. *J. Phys. II* **1994**, *4*, 2161.
(26) Förster, S.; Khandpur, A. K.; Zhao, J.; Bates, F. S.; Hamley, I. W.; Ryan, A. J. *Macromolecules* **1994**, *27*, 6922.
(27) Khandpur, A. K.; Förster, S.; Bates, F. S.; Hamley, I. W.; Ryan, A. J.; Bras, W.; Almdal, K.; Mortensen, K. *Macromolecules* **1995**, *28*, 8796.
(28) Schulz, M. F.; Khandpur, A. K.; Bates, F. S.; Almdal, K.; Mortensen, K.; Hajduk, D. A.; Gruner, S. M. *Macromolecules* **1996**, *29*, 2857.
(29) Almdal, K.; Mortensen, K.; Ryan, A. J.; Bates, F. S. *Macromolecules* **1996**, *29*, 5940.
(30) Vigild, M. E.; Ndoni, S.; Almdal, K.; Hamley, I. W.; Fairclough, J. P. A.; Ryan, A. J. Phase Behavior of Poly(ethylene-*co*-propylene)−polydimethylsiloxane (PEP−PDMS) Copolymers. In preparation.
(31) Hillmyer, M. A.; Bates, F. S.; Almdal, K.; Mortensen, K.; Ryan, A. J.; Fairclough, J. P. A. *Science* **1996**, *271*, 976.
(32) Hillmyer, M. A.; Bates, F. S. *Macromolecules* **1996**, *29*, 6994.
(33) Matsen, M. W.; Bates, F. S. *Macromolecules* **1995**, *28*, 7298.
(34) Qi, S.; Wang, Z.-G. *Phys. Rev. Lett.* **1996**, *76*, 1679.
(35) Qi, S.; Wang, Z.-G. *Phys. Rev. E* **1997**, *55*, 1682.
(36) Shi, A.-C.; Noolandi, J.; Desai, R. C. *Macromolecules* **1996**, *29*, 6487.
(37) Laradji, M.; Shi, A.-C.; Desai, R. C.; Noolandi, J. *Phys. Rev. Lett.* **1997**, *78 (*13*)*, 2577.
(38) Fredrickson, G. H.; Helfand, E. *J. Chem. Phys.* **1987**, *87*, 697.
(39) Lipic, P. M.; Zhao, J.; Matsen, M. W.; Hajduk, D. A.; Kossuth, M. B.; Bates, F. S. Kinetic Trapping of Nonequilibrium Morphologies in Polyethylene−Poly(ethylethylene) Block Copolymers. In preparation.

MA961673Y